

# Stress corrosion crack propagation in glass fibre reinforced/thermoplastic PET

KLAUS FRIEDRICH\*

*Institute for Materials Science, Ruhr-University Bochum, 4630 Bochum, West Germany*

This study covers results of stress rupture tests obtained with compact tension specimens of a glass fibre/thermoplastic matrix composite in chemical environments at room temperature. The corrosive media used were various acidic solutions. All the tests indicate a deterioration of the crack resistances of the materials to a greater or lesser extent, under environmental attack, i.e. cracks can propagate faster than in water or air. This particular behaviour is also influenced by microstructural parameters, i.e. fibre fraction and the local orientation of fibres to the propagating crack. In all cases, most attack occurs at the fibre–matrix interfaces and at the fibres, while the matrix is insensitive to the aggressive medium. The results are discussed in terms of crack growth rate,  $da/dt$ , and threshold fracture toughness value,  $K_{SCC}$ , below which statically loaded structural components are expected to have infinite life when subjected to a particular test environment.

## 1. Introduction

Fibre reinforced plastic (FRP) materials are often used to provide corrosion resistance in applications where metals or alloys are either unsuitable or costly. Nevertheless, it has been established, at least qualitatively, that FRP can be severely weakened in the presence of moisture or other aggressive environments, and it is interesting to consider the possible causes for this [1–3]. In composites, the polymer–glass interface and the glass fibre reinforcement are considered to be more susceptible to environmental degradation than the polymer matrix material [4, 5]. Thus, the matrix usually serves to protect the interface and the fibres from attack. However, if the aggressive medium can travel through the polymer, either by diffusion or microcracks, corrosion of the interface and the fibres can occur.

In this paper some important corrosion mechanisms will be discussed, which have been recently investigated in studies of the stress corrosion crack resistance of a commercial short glass fibre/polyethylene terephthalate system (Rynite<sup>®†</sup>).

The compositions of Rynite<sup>®</sup> with 30 or 45 wt% glass reinforcement belong to the group of fibre reinforced thermoplastics with the highest stiffness. They can be processed in standard injection moulding machines without any problems. These and various other advantages of Rynite<sup>®</sup> have led to advanced technical application of this composite material in the automotive industry [6]. For this application, on the other hand, a good knowledge about the mechanical performance on the composite, especially its failure behaviour under loading conditions in more or less aggressive environments, is very important.

## 2. Experimental procedure

### 2.1. Test method

Much of the previous work has been restricted to environmental exposure of the composite followed by mechanical testing, although in many cases the application of load and environment occur simultaneously. As the presence of an applied stress can significantly affect the environmental degradation, in this study the material is tested using one of the

\* This work was carried out by the author during a research stay at the Centre for Composite Materials, University of Delaware, Newark, Del. 19711, USA.

† Registered trademark of E.I. du Pont de Nemours and Co., Inc.

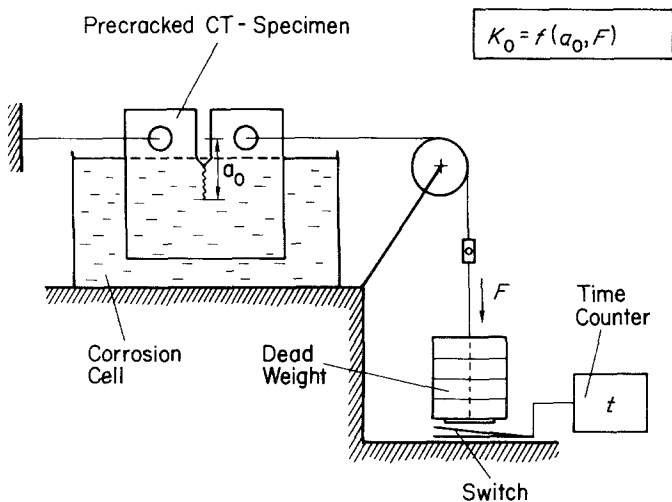


Figure 1 Schematic diagram of the equipment for environmental stress rupture tests.

successfully developed fracture mechanics approaches for studies of stress corrosion cracking in metallic materials [7, 8].

This concept is based on the determination of a stress corrosion cracking,  $K_{ISCC}$ , threshold value, first introduced by Brown [9]. Usually, precracked specimens are monotonically loaded to failure in a certain environment using a stand similar to that shown in Fig. 1. Subsequently, the dead-weight load is successively reduced to lower initial stress intensity factor,  $K_{I0}$ , levels. As long as the crack length increases under these constant loads, the stress intensity factor at the crack tip increases to the critical stress intensity,  $K_{Ic}$ , level and the specimen fractures. The lower the value of the initial  $K_{I0}$ , the longer the time to failure (Fig. 2). Finally, when a plane strain  $K_{I0}$  level is reached at which crack extension does not occur even after a long test time, this value corresponds to the stress

corrosion cracking threshold,  $K_{ISCC}$ . Thus,  $K_{ISCC}$ , for a given material and environment, corresponds to the plane strain stress intensity factor below which statically loaded structural components are expected to have infinite life when subjected to the particular test environment.

Fig. 3 is a schematic representation of the test results obtained by using a more or less aggressive medium during the test. Approximately ten precracked specimens are needed to establish  $K_{ISCC}$  for a particular material and environment. It has to be mentioned that in the present work no valid  $K_{ISCC}$  data are determined, i.e. values under real plane strain conditions, due to the lack of specimen thickness. Therefore, the index "I", which stands for crack opening Mode I under plain strain conditions, is left out in the diagrams of Figs 2 and 3. However, the measurements are useful for observing the tendencies which occur when these

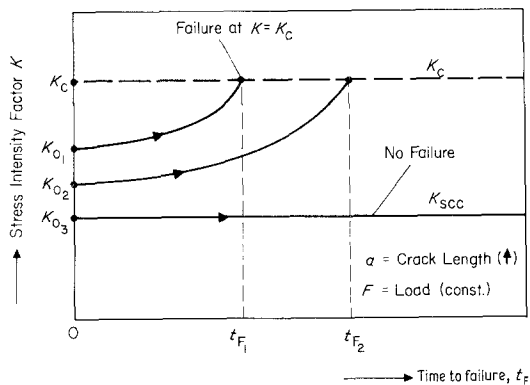


Figure 2 Change in  $K$  value associated with subcritical flaw growth. Regardless of  $K_0$ , failure in any sample occurred at  $K = K_c$ .

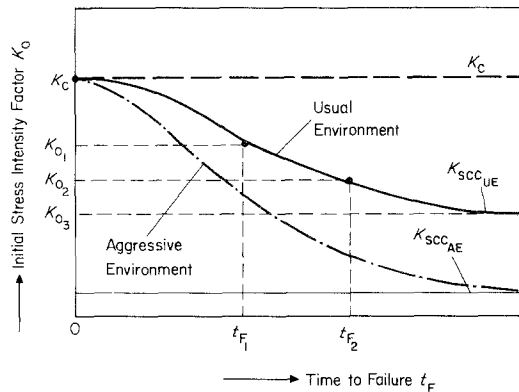


Figure 3 Procedure for obtaining  $K_{SICC}$  with CT-specimens tested under various initial stress intensity conditions in various environments.

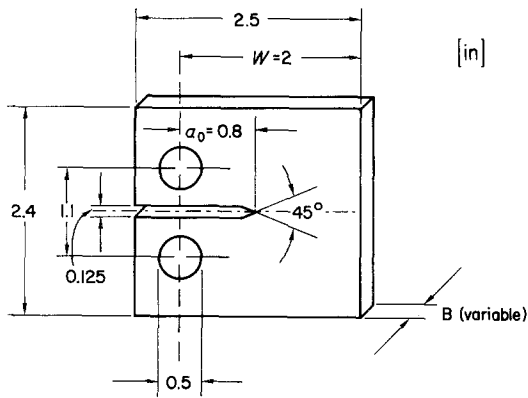


Figure 4 CT-specimen configuration.

materials are stressed under various corrosive conditions.

The following environments were used in this study: laboratory air, laboratory water and three aqueous solutions containing 3 vol% HCl, 10 vol% HCl and 3 vol% H<sub>2</sub>SO<sub>4</sub>, respectively. All tests were carried out using compact tension (CT)-specimens (Fig. 4). During the tests the specimens were unloaded from time to time in order to measure the actual amount of crack growth. Thus crack growth rate data were obtained which should provide information necessary for enhancing the understanding of the kinetics of stress corrosion cracking and to verify the threshold behaviour,  $K_{I\text{SCC}}$ .

## 2.2. Materials

In the present case, the composite consists of short E-glass fibres dispersed in a thermoplastic polyethylene terephthalate (PET) matrix, specifically formulated for rapid crystallization. Two compositions were injection moulded into end-gated rectangular plaques: Rynite<sup>®</sup> 545-I, a 45 wt% glass/PET compound, and Rynite<sup>®</sup> 530-I containing 30 wt% short glass fibres. Scanning electron microscopic studies show that the glass fibres are aligned in "boundary layers" near the mould surface, and are distributed perpendicular to the mould fill direction in the interior of the plaques (Fig. 5). The size of the layers and degree of fibre orientation depend on plaque thickness [10] and fibre fraction [11]. Since the fibre alignment yields highly anisotropic mechanical properties, the plaques were tested in two directions (Fig. 6): once with crack growth transverse to the dominant fibre orientation at the surfaces (T-cracks); and once with crack growth nearly parallel to the mould fill

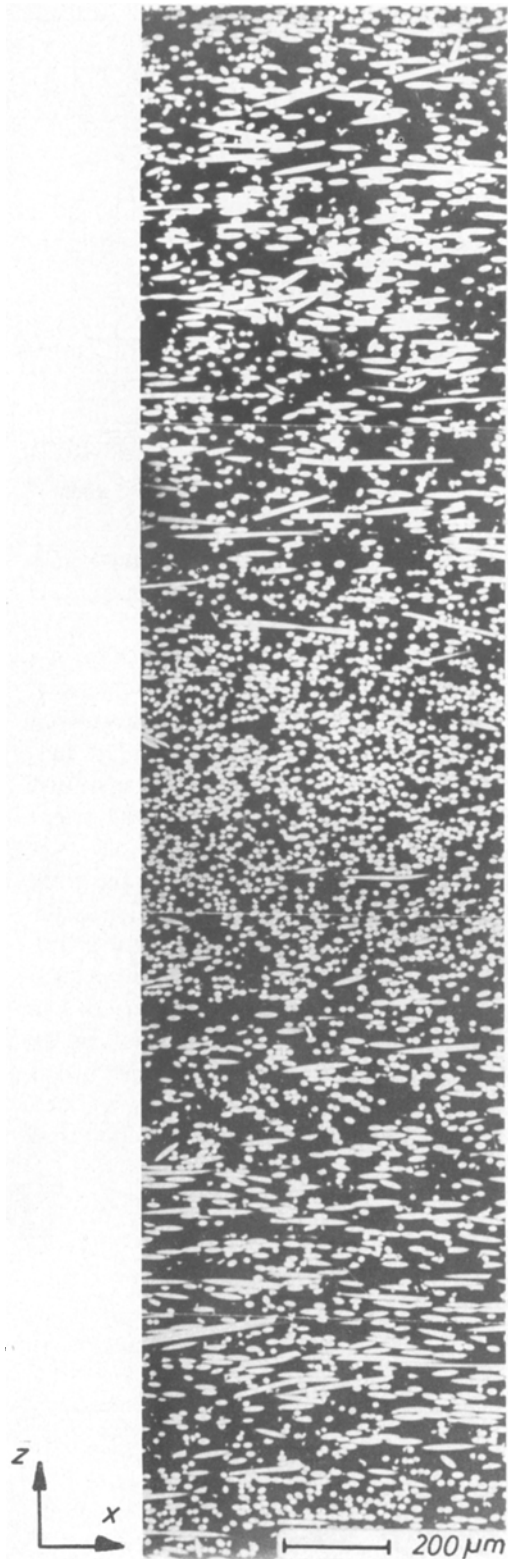


Figure 5 Scanning electron micrograph of the fibre distribution across the plaque thickness 3.2 mm of Rynite<sup>®</sup> 545-I (X-Z plane, cf. Fig. 6).

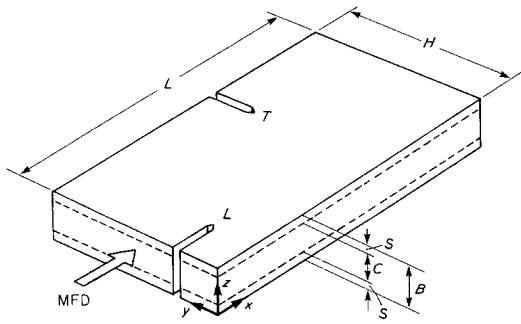


Figure 6 Direction of L- and T-cracks with respect to plaque geometry.

direction MFD (longitudinal fibre orientation, L-cracks).

### 3. Results and discussion

#### 3.1. Stress intensity–time to failure curves

Fig. 7 shows the results of the stress rupture tests with Rynite® 545-I, L-direction, obtained in air, water and three acidic environments, 3 vol% and 10 vol% HCl and 3 vol% H<sub>2</sub>SO<sub>4</sub>. The time to failure curves can be divided into three stages:

In Stage I the data points lie in the scatter bar

of the fracture toughness usually determined in air by monotonically increasing load to fracture. These specimens fail by a relatively fast, subcritical crack propagation under the initial viscoelastic/plastic response of the material to the applied load without being affected by the environment used.

Stage II shows an approximately linear decrease of the initial fracture toughness necessary to induce crack growth and final fracture after a certain time. During this stage further crack growth will nucleate at the tip of the machined precrack under strain corrosion conditions. The time to initiate this mechanism depends on the kind of corrosive environment. In air Stage II occurs after a much longer time than when testing the specimens in acidic aqueous solutions. Especially in 10 vol% HCl and 3 vol% H<sub>2</sub>SO<sub>4</sub> solutions, the decrease of the necessary stress intensity level to initiate stress corrosion cracking was found to be in the range of  $5 \times 10^3$  sec. On the other hand, the data obtained in water environment fell close to the scatter band of the in-air data. The effect of water alone is thus seen to be different from that of the aqueous acids studied, which was also

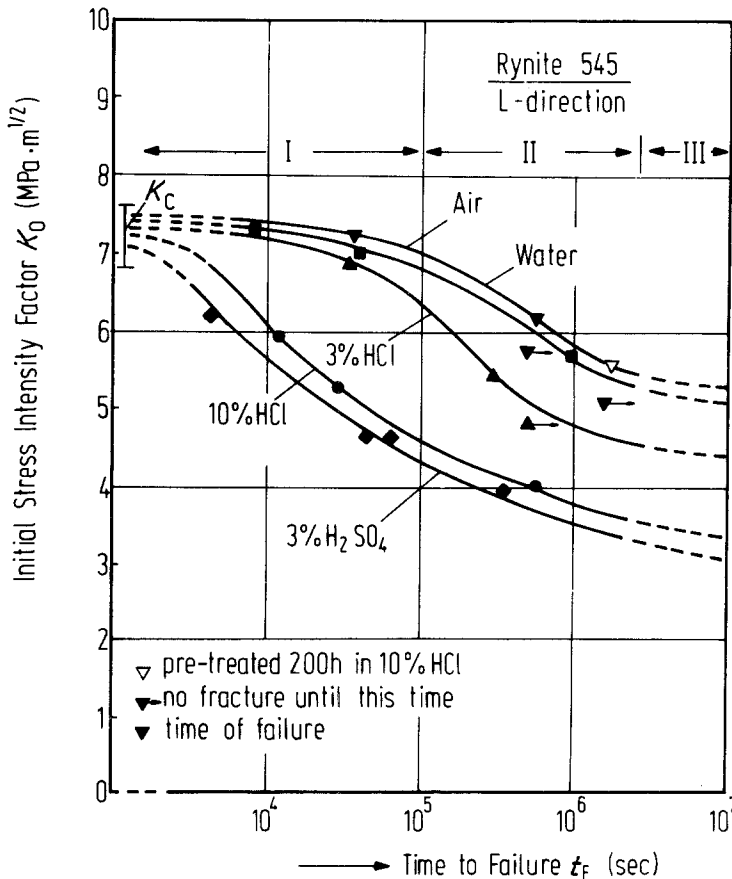


Figure 7 Initial stress intensity–time to failure curves for Rynite® 545-I, L-direction, in various environments.

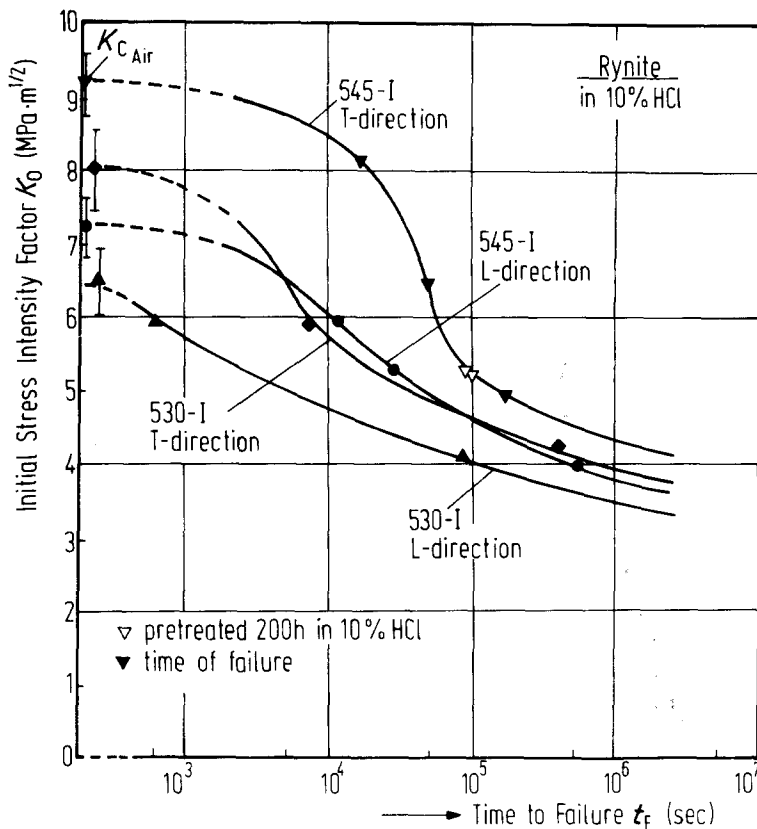


Figure 8 Initial stress intensity-time to failure curves for the L- and T-directions in Rynite® 545-I and 530-I obtained in 10 vol% HCl.

found by Carswell and Roberts [12] for the fatigue stress corrosion failure of glass fibre reinforced polyester.

In Stage III the data points seem to approach a certain stress intensity level for very long testing under which corrosive cracking cannot be initiated. However, due to the short time available for these investigations this level could not be determined exactly. But it can be seen from the tendency of the data points that failure in the acidic environments occurs at much lower stress intensity levels than in air. This indicates different  $K_{SCC}$  values for the particular environments.

More comprehensive data from the hydrochloric acid tests are given in Fig. 8 for Rynite® 545-I, T-direction and both directions in Rynite® 530-I. In Stage I the difference between the time to failure curves is relatively high due to different stress intensity factors,  $K_C$ , for the various materials and crack directions. At lower stress intensity levels (endurance greater than about  $10^5$  sec), on the other hand, the curves fall within a fairly narrow band. This is due to the fact that the T-cracked specimens express a much steeper decrease of the  $K_0$  values necessary to induce stress corrosion failure in Stage II than the L-

cracked specimens. This increase in degradation seems to be due to the fact that the higher amount of fibre fracture responsible for the higher fracture toughness of the T-cracked as compared to the L-cracked specimens has changed into fibre pull-out failure after enhanced degradation of the interfaces.

There are two additional points about Figs 7 and 8. Specimens which were pretreated for 200 h in 10 vol% HCl solution at room temperature without exposure to an external stress were then loaded either in air (545-I, L-direction) or in 10 vol% HCl (545-I, T-direction). In both cases no significant influence of the pretreatment could be observed. This shows that chemical attack during immersion (in at least 10 vol% HCl) does not normally cause serious loss of the physical properties, but that a combination of chemical and mechanical interaction between the composite and the environment leads to rapid deterioration. A similar result was shown by Hojo and Tsuda [13] for environmental stress cracking of glass fibre reinforced vinyl ester resin in 10 vol% HCl. Andrews [14] has also pointed out that it is the combination of chemical and physical factors that normally causes localized attack in composite

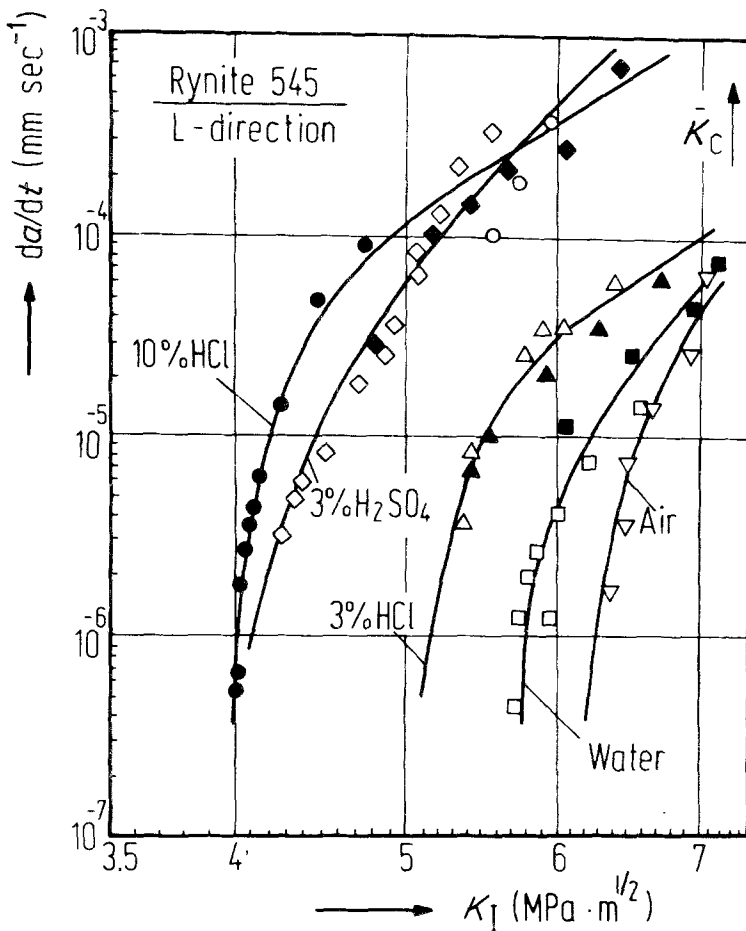


Figure 9 Stress corrosion crack velocity against stress intensity factor for Rynite® 545-I in various environments. Different symbols refer to different specimens.

materials. Consequently, it can be concluded from these results that the transition time from the first to the second degradation stage, which appears in the stress intensity-time curves, represents the initiation time of the chemical degradation at the glass-matrix interface under stress. Once the interface is stressed, it can, on the one hand, act as a pathway through which the aggressive medium can penetrate in order to induce dissolution and disruption of the glass fibres. On the other hand, degradation of the interfacial matter itself can occur much more easily due to a higher amount of surface produced by the local stresses.

### 3.2. Crack growth measurements

The results of the crack growth measurements shown in Figs 9 and 10 give an idea about the crack growth kinetics in the various environments. The measurements can be partly described by a power relationship of the form

$$da/dt = \alpha \cdot K_I^m, \quad (1)$$

where  $\alpha$  and  $m$  are material constants, which also

depend on the particular environment and other testing conditions [2],  $a$  is crack length and  $t$  is time. Equation 1 often holds over several decades of  $da/dt$  but at very low values the velocity is sometimes observed to fall rapidly with a decrease in  $K_I$  towards a stress corrosion limit,  $K_{I,SCC}$ . In particular, the diagrams illustrate the following results:

(1) Crack propagation under stress rupture conditions can be initiated at lower  $K_I$  values in acidic environments. The environment reduces the stress corrosion limit in the following order: 3 vol%  $H_2SO_4 \approx 10$  vol%  $HCl > 3$  vol%  $HCl > H_2O > air$ .

(2) The same sequence is given for the crack propagation velocity at a given  $K_I$  level, i.e. in the aqueous, more or less acidic solutions cracks propagate faster than in air. In this connection it should be mentioned that the higher crack growth rate for the specimens tested in water compared with those tested in air are in opposition to the results observed by Mandell [15] for moisture effects on crack propagation in reinforced polyester.

(3) Cracks grow more slowly in T-cracks than in

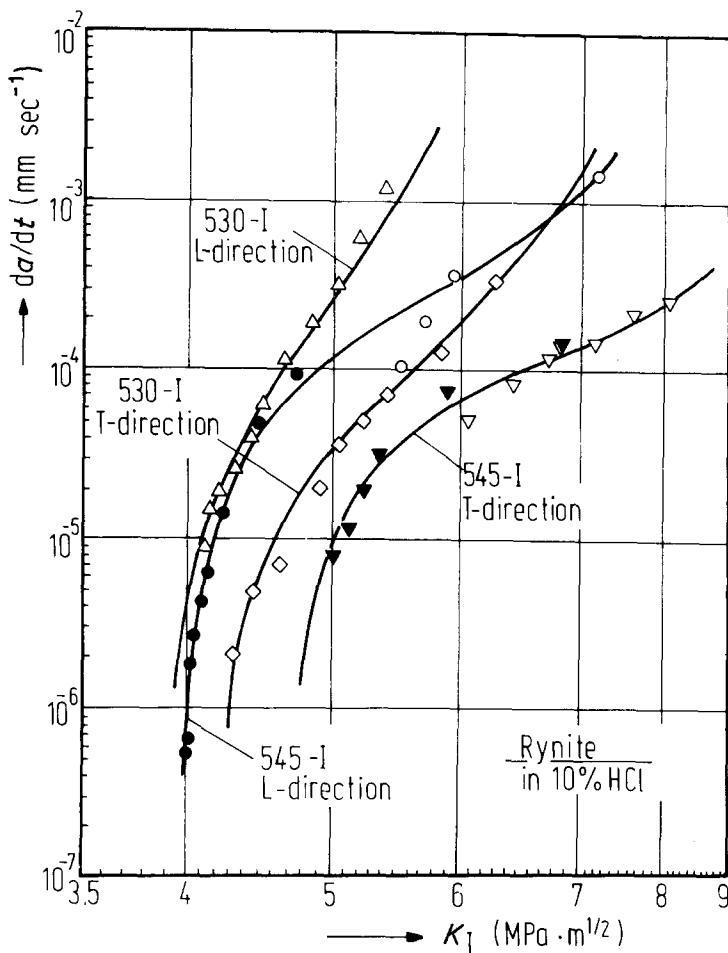


Figure 10 Environment assisted cracking in 10vol% HCl solution for different crack directions and fibre fractions in Rynite®.

L-cracks and slower in Rynite® 545-I than in 530-I. However, all these curves start in a narrow range of  $K_I$  between 3.9 and 4.7  $\text{MPa}\cdot\text{m}^{1/2}$ . This may be expected from the results shown in Fig. 8.

### 3.3. Microscopic analysis of the SCC mechanisms

Fractographic studies on composite materials tested under stress corrosion conditions show many different failure phenomena which can be related to the particular materials and the testing environments [3, 5, 12, 13, 16–18]. They have, however, some things in common: a higher degradation of the fibre–matrix interfaces and a higher amount of fibre failure due to the attack of the aggressive environment. In addition, sometimes chemical reactions between the environment and the matrix material are observed.

In the present study one of the most aggressive media with respect to the degradation of the mechanical properties was 10vol% HCl. Therefore its influence on the fracture surface characteristics

was analysed first. Fig. 11 compares the appearance of representative L-cracked areas in Rynite® 545-I taken from an in-air produced crack and a crack developed under stress corrosion conditions. The fibres on the fracture surface of the in-air cracked specimens are still well bonded and show the typical stretched polymer tips on their surfaces (Fig. 11a). The stress corroded area, on the other hand, shows many debonded fibres (Fig. 11b). They look very similar to those found on the fracture surface of a poorly bonded system when broken under normal environmental conditions [11]. This indicates that, at least to a certain degree, the interface is the crucial parameter. Hojo and Tsuda [13] showed that the degradation of this microstructural element is especially accelerated in HCl. It should be noted, however, that it was not easy in this study to distinguish these differences of the cracked areas on a first view with the scanning electron microscope (SEM), although a clear difference between them could be seen with the naked eye. The corroded fracture

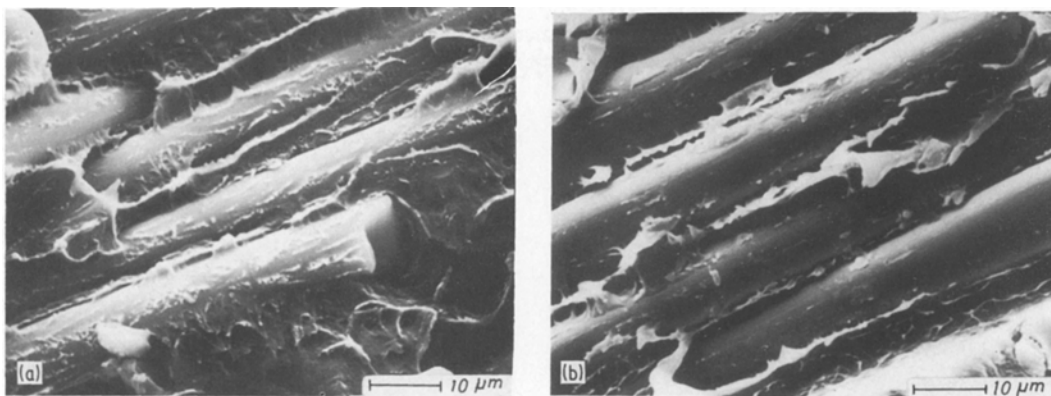


*Figure 11* Fracture surfaces showing (a) polymer adhering to the glass fibres in a specimen fractured in air and (b) weak adhesion between fibres and matrix in a region of stress corrosion crack growth in 10 vol% HCl.

parts looked much smoother than both the corresponding areas of in-air cracked specimens and the transitional and final regions of rapid crack propagation.

Fig. 12a and b represent typical zones taken from a specimen which was broken under low stress intensity—long time to failure conditions in 3 vol%  $H_2SO_4$ . In this case the fibres aligned in the L- and T-directions are still coated with some stretched polymer tips but show a lot of ring- or helix-shaped cracks on their surfaces. That means that the process of enhanced interfacial fracture was supported by the interaction between the E-glass and the acid. In fact, several authors have shown that during the corrosion process an exchange between surface ions of the glass and hydrogen ions can cause volume changes which are able to produce surface tensile stresses on the fibres. These stresses were shown to be capable of

developing to levels sufficiently high to bring about spontaneous cracking of the fibres [5, 17–19]. The formation of these cracks can occur even in the absence of an applied stress. This is indicated in Fig. 13 for a poorly bonded glass fibre/PET matrix system. The fracture surface of an in-air broken specimen (Fig. 13a) contains completely debonded fibres with film-like stretched matrix segments between them. When these fibres are subsequently exposed to a 3 vol%  $H_2SO_4$  solution for one week, multiple cracking of the fibres can be observed (Fig. 13b). As these cracks can also form in loaded specimens under environmental exposure, the fibres do no longer contribute to the materials crack resistance so that macroscopic cracks can propagate very rapidly through the composite.

Finally it should be mentioned that, at least in this study, no degradation effects of the

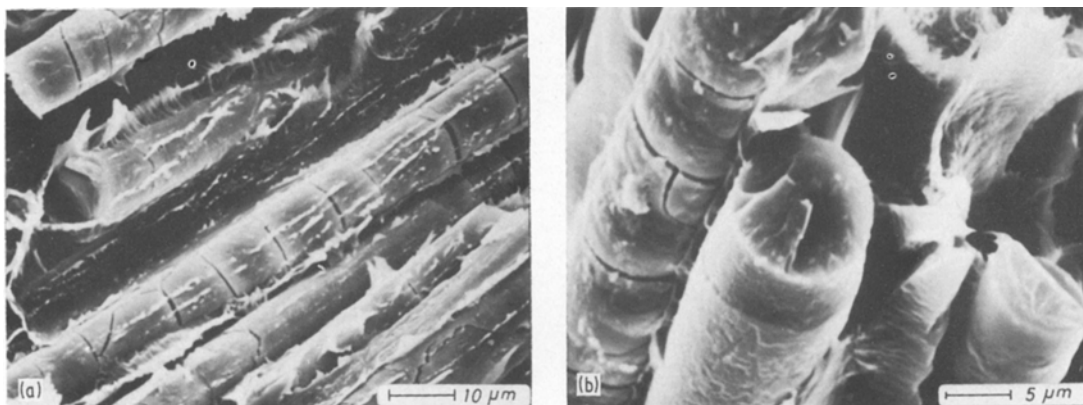


*Figure 12* (a) Multiple cracking of fibres lying perpendicular to the applied load resulting from additional chemical attack by 3 vol%  $H_2SO_4$  solution and (b) surface degradation and cracking of fibres transversely oriented to the main crack direction.



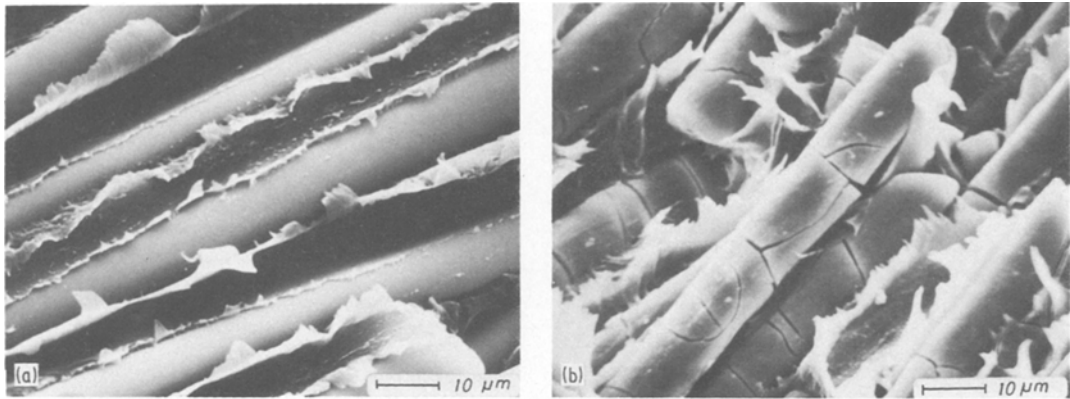


Figure 13 Fracture surfaces of a poorly bonded glass fibre/PET system: (a) broken in air and (b) broken in air and then treated in 3 vol%  $H_2SO_4$  leading to multiple fibre cracking.

thermoplastic PET matrix by the acidic solutions were noticed. Even after  $3.5 \times 10^5$  sec under an initial stress intensity factor of  $K_{I0} = 1.7 \text{ MPa m}^{-1/2}$  (this is about 77% of the critical stress intensity factor of the matrix material) no remarkable crack growth could be detected. On the contrary, a 1.7-fold higher load than necessary for breaking the plaques directly in air was needed in a subsequent fracture mechanics test to pull the immersed specimen apart. The observed increase in fracture toughness seems to be due to a blunting of the crack tip during immersion on the aqueous solution under low stress. The blunting effect can be recognized indirectly on the final fracture surface of the broken specimen in the region of the machined notch tip (Fig. 14a and b). A 2-fold higher step is measured in the case of the immersed specimen compared with the in-air cracked sample.

Assuming that all these observations are typical effects for the attack of glass fibre reinforced PET, a model can be established which describes the individual phenomena schematically (Fig. 15):

(1) In general, crack propagation through a short fibre thermoplastic matrix system under external load,  $\sigma$ , is dominated by three basic mechanisms: (a) plastic deformation and final failure of the matrix; (b) fibre–matrix debonding, including fibre pull-out; and (c) fibre fracture.

(2) The contribution of energy absorbed by these individual mechanisms to the materials crack resistance depends on the local orientation of the fibres to the propagating crack as well as the partial properties of the three microstructural elements: matrix, fibre and fibre–matrix interface.

(3) If some of these partial properties are reduced by any kind of environmental attack

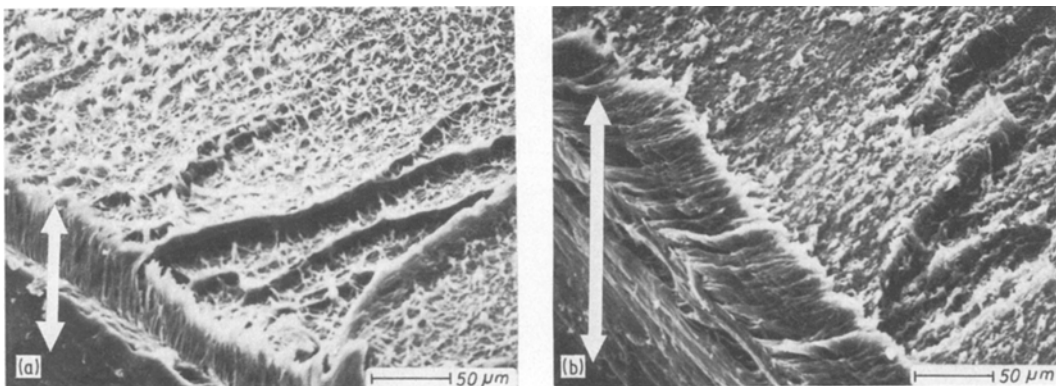


Figure 14 Variation of crack initiation mode, in the pure matrix material, with environmental and testing conditions: (a) crack acceleration through a plane deformed by some crazes under monotonically increased load in air and (b) blunting of the notch tip and multiple void formation in the plastic zone in front of the notch under stress rupture conditions in acidic solution.

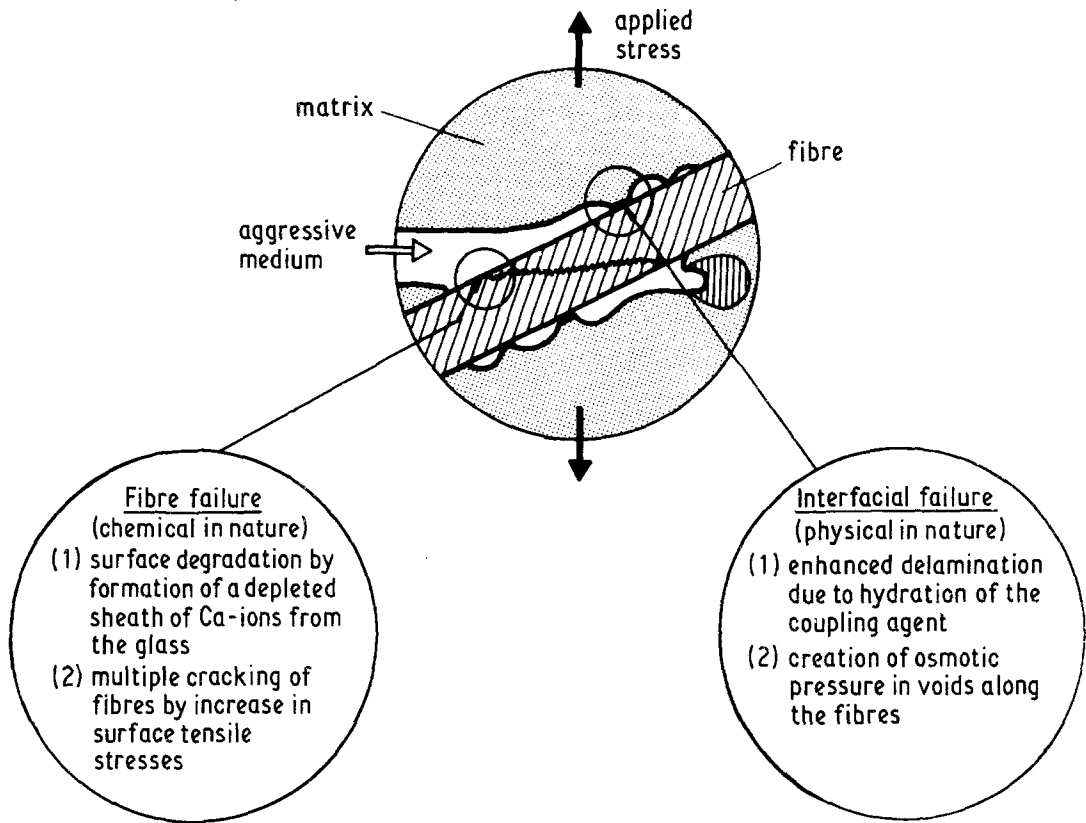


Figure 15 Schematic diagram of local failure mechanism in a glass fibre reinforced/thermoplastic matrix system under environmental attack.

crack propagation and fracture along these micro-structural elements is favoured.

(4) In the cases of water and aqueous hydrochloric acid solutions a significant corrosion mechanism, physical in nature, is most likely occurring at the fibre–matrix interfaces. Once the external load has involved penetration of the liquid into the plastically deformed region around the tip of the notch, subsequent adsorption of the liquid at the glass fibre–polymer interfaces occurs. This promotes the destruction of the mechanical (or chemical, if any) bonds between the glass fibre and the polymer and results in loss of physical properties. The extent to which the above described reactions occur depends on the strength of the aggressive medium used, as shown by the more detrimental effect of the 10 vol% HCl compared with the 3 vol% HCl or the pure aqueous solutions.

(5) Another distinct reduction of the mechanical properties of the composite can occur when the glass fibres are dissolved by the acidic environment used. As soon as the applied mechanical stress has caused void formation along the fibres the acid can penetrate with increasing rate into the

laminate. Subsequently the exposed glass fibres will be attacked by the acid and fracture resulting in stress corrosion crack propagation.

### Acknowledgement

I am grateful to Professor J. M. Schultz and Professor R. B. Pipes, Centre for Composite Materials, University of Delaware and to Dr E. Dyrup and Dr B. Epstein of E.I. du Pont de Nemours and Co. Inc., for supporting this endeavour and for many helpful discussions. The help of Mr Chang Lhynn during the SCC measurements is also appreciated. The research stay at the University of Delaware was supported by the Alexander-von-Humboldt-Foundation (AvH), which is gratefully acknowledged.

### References

1. R. C. ALLEN, *Polymer Eng. Sci.* 19 (1979) 329.
2. J. AVESTON, Proceedings of the 3rd International Conference on Composite Materials, Vol. 1, Paris 1980 (Pergamon Press, Oxford, 1980) p. 556.
3. D. HULL and P. J. HOGG, *ibid.* p.543.
4. J. C. HAARSMA, paper 22-E, Proceedings of the 34th Annual Conference on Reinforced Plastics/

- Composites (Institute of the Society of the Plastics Industry, New Orleans, 1979).
5. S. TORP and R. ARVESEN, *ibid.* paper 13-D.
  6. J. D. YOUNG, *Technica* 18 (1980) 1515.
  7. S. T. ROLFE, "Fracture and Fatigue Control in Structures", (Prentice-Hall, Inc., Englewood Cliffs, New Jersey, 1977).
  8. R. NOVAK and S. T. ROLFE, *J. Mater.* 4 (1969) 701.
  9. B. F. BROWN, *Mater. Res. Stand.* 6 (1966) 129.
  10. R. C. WETHERHOLD, W. A. DICK and R. B. PIPES, SAE Technical Paper number 800812 (Society of Automotive Engineers, Warrendale, Pennsylvania, 1980).
  11. K. FRIEDRICH, *Practical Metallography* (1981) in press.
  12. W. S. CARSWELL and R. C. ROBERTS, *Composites* 11 (1980) 95.
  13. H. HAJO and K. TSUDA, paper 13-B, Proceedings of the 34th Annual Conference on Reinforced Plastics/Composites (Institute of the Society of Plastics Industry, New Orleans, 1979).
  14. E. H. ANDREWS, *Brit. Polymer J.* 10 (1978) 39.
  15. J. F. MANDELL, *Polymer Eng. Sci.* 19 (1979) 353.
  16. B. DEWIMILLE, J. THORIS, R. MAILFERT and A. R. BUNSELL, Proceedings of the 3rd International Conference on Composite Materials, Vol. 1, Paris 1980 (Pergamon Press, Oxford, 1980) p. 597.
  17. J. E. BAILE, T. M. W. FRYER and F. R. JONES, *ibid.* p. 515.
  18. L. S. NORWOOD and A. F. MILLMANN, paper 3-D, Proceedings of the 34th Annual Conference Reinforced Plastics/Composites (Institute of the Society of Plastics Industry, New Orleans, 1979).
  19. G. W. SCHMITZ and A. G. METCALFE, *Ind. Eng. Chem. Prod. Res. Dev.* 5 (1966) 1.

Received 27 February and accepted 30 April 1981.